Biochemical Pharmacology, Vol. 35, No. 7, pp. 1071–1078, 1986.
Printed in Great Britain.

0006-2952/86 $3.00 + 0.00

IDENTIFICATION OF THE ACTIVE SPECIES IN DEOXYRIBONUCLEIC ACID BREAKAGE INDUCED BY 4′-(9-ACRIDINYLAMINO)METHANESULFON-*m*-ANISIDIDE AND COPPER

ANGELA WONG,*† HUNG-YUAN CHENG‡ and STANLEY T. CROOKE†

† Department of Molecular Pharmacology and ‡ Department of Analytical, Physical and Structural Chemistry, Smith Kline & French Laboratories, Philadelphia, PA 19101, U.S.A.

(*Received* 18 *April* 1985; *accepted* 15 *August* 1985)

Abstract—Cyclic voltammetry and UV/VIS spectrometry studies show that 4′-(9-acridinylamino)-methanesulfon-*m*-anisidide (mAMSA) can be oxidized electrochemically to N^1-methylsulfonyl-N^4-(9-acridinyl)-3-methoxy-2,5-cyclohexadiene-1,4-diimine (mAQDI) in Tris buffer, pH 7.5. The formal potential of this 2-electron process, as determined by spectroelectrochemical techniques, was 0.141 V versus saturated calomel electrode. Voltammetric data also indicate that an electron transfer reaction between mAMSA and Cu(II) was thermodynamically favored. Two lines of evidence suggest that mAQDI and Cu(I) are the active species in DNA breakage: (1) mAQDI, in the presence of Cu(I), induced both single- and double-strand DNA breakage of the superhelical pDPT275 form I DNA. mAQDI or Cu(I), when used alone, was less effective. (2) The DNA-breaking activity of an mAMSA–Cu(II) mixture was kinetically correlated with the production of both Cu(I) and mAQDI. Thin-layer chromatographic studies showed that mAMSA was oxidized to mAQDI which, in turn, was hydrolyzed. The end product was identified as 9-aminoacridine. When DNA breakage activity was measured as a function of reaction time, a biphasic response was observed. Maximal DNA-breaking activity was obtained upon mixing mAMSA and Cu(II) for 2–4 hr, depending on the concentrations of mAMSA and Cu(II), and was followed by a subsequent decrease in breakage. The decrease appears to be due to the decrease in Cu(I) production and the hydrolysis of mAQDI. These results substantiate the proposed mechanism that DNA breakage induced by mAMSA–Cu(II) involves a rate-limiting electron transfer step to form mAQDI and Cu(I), which are the active species for DNA breakages.

4′ - (9 - Acridinylamino) - methanesulfon - *m* - anisidide (mAMSA)§, a 9-aminoacridine derivative developed by Cain and Atwell [1], is currently undergoing Phase II to III clinical trials to determine its possible usefulness as an antitumor drug. mAMSA is highly active against human acute leukemia [2, 3]. It is also effective in treating lymphomas [4] and carcinoma of the breast [5]. The mechanism by which the drug exhibits its cytotoxic activities is not understood, but its strong DNA-intercalating properties suggest that the drug receptor site may be DNA [6]. There is a close relationship between chromosome breakage and cytotoxic potency of a range of mAMSA analogues, indicating that chromosome breakage may be responsible for the cytotoxic effect of mAMSA [7]. mAMSA may induce DNA single-strand breaks, double-strand breaks, as well as DNA protein cross-links in L1210 leukemia cells [8].

We have demonstrated previously that mAMSA, in the presence of Cu(II) ion, induces *in vitro* breakage of the plasmid pDPT275 and pBR322 superhelical form I DNA [9]. mAMSA is oxidized by Cu(II), resulting in the production of a quinodal diimine, mAQDI (N^1-methylsulfonyl-N^4-(9-acridinyl)-3-methoxy-2,5-cyclohexadiene-1,4-diimine) and Cu(I) ion [10]. We have proposed that a DNA–mAQDI–Cu(I) ternary complex may be formed. Cu(I) may then be reoxidized to Cu(II) by reducing molecular oxygen and, in the process, generating a variety of oxygen free radicals which may induce DNA breakage. Since mAMSA binds to DNA by intercalation of the acridine chromophore between adjacent base pairs, the formation of the ternary complex may reduce the diffusion distance from the site of free radical generation to the targets in DNA and enhance the cutting efficiency.

In the studies reported here, we have employed cyclic voltammetry and spectroelectrochemical methods to investigate the mAMSA–Cu(II) redox system. These techniques provide valuable information on the redox potentials, stability and reaction mechanism. Furthermore, by using controlled potential electrolysis, we are able to generate high purity mAQDI *in situ*. We have demonstrated that mAQDI and Cu(I) are the active species for DNA breakage and substantiated the proposed mechanism [10] that

* Reprint requests should be addressed to: A. Wong, Smith Kline & French Laboratories, L-108, P.O. Box 7929, Philadelphia, PA 19101.

§ Abbreviations: bathocuproine, 2,9-dimethyl-4,7-diphenyl-1,10-phenanthroline; DNA, deoxyribonucleic acid; $E^{\circ\prime}$, formal reduction potential; mAMSA, 4′-(9-acridinylamino)-methanesulfon-*m*-anisidide; mAQDI, N^1-methylsulfonyl-N^4-(9-acridinyl)-3-methoxy-2,5-cyclohexadiene-1,4-diimine; mAQI, 3′-methoxy-4′-(9-acridinylamino)-2′,5′-cyclohexadiene-1′-one; *n*, number of electrons transferred; OTTLE, optically transparent thin-layer electrode; RVC, reticulated vitreous carbon electrode; S.C.E., saturated calomel electrode; and Tris, tris(hydroxymethyl)aminomethane.

DNA breakage by mAMSA–Cu(II) involves an initial rate-limiting redox reaction to form the oxidized drug (mAQDI) and the reduced metal [Cu(I)].

MATERIALS AND METHODS

Materials. mAMSA was supplied by Bristol Laboratories, Syracuse, NY. mAMSA was dissolved in dimethyl sulfoxide (3 mg/ml) and diluted with distilled water to 1 mg/ml. The final concentration of dimethyl sulfoxide in the DNA reaction mixture was 2–3%. pDPT275 plasmid is a second step copy number mutant derived from R100(NRI) plasmid. It was isolated according to the procedure of Clewell and Helinski [11]. 9-Aminoacridine, bathocuproine disulfonate, bromophenol blue, dimethyl sulfoxide, Na_2EDTA, ethidium bromide, $CuSO_4 \cdot 5H_2O$, glycerol, sodium citrate, sodium phosphate, and Tris were obtained from the Sigma Chemical Co., St. Louis, MO. Benzene was obtained from Beckman Instruments, Palo Alto, CA. CuCl and silica gel IB2F plates (20 × 20 cm, 0.1 mm thickness) were purchased from the J. T. Baker Chemical Co., Phillipsburg, NJ. Agarose-ME was obtained from Bethesda Research Laboratories, Gaithersburg, MD.

Determination of drug and DNA concentrations. The concentrations of mAMSA and DNA were determined spectrophotometrically. For mAMSA, a molar extinction coefficient of 1.20×10^4 cm^{-1} at 434 nm (in water) was used [12]. A molar extinction coefficient of 6600 $cm^{-1} M^{-1}$ (at 260 nm) was used for pDPT275 plasmid DNA in aqueous solutions.

Electrochemical experiments. The conventional three electrode system was used throughout this study. The potentiostat used was a model 174A polarographic unit from Princeton Applied Research/EG and G, Princeton, NJ. All redox potentials reported are measured versus a saturated calomel reference electrode (S.C.E.). Cyclic voltammetry was performed with a carbon paste working electrode. Control potential electrolysis was carried out with a cylindrical reticulated vitreous carbon (RVC) electrode of 2 cm long and 0.5 cm in diameter. A platinum wire was glued to the top of the cylinder with a graphite/epoxy mixture to provide the necessary electrical contact. The dimension of the working electrode compartment of the divided electrolytic cell was only slightly larger than the porous RVC electrode so that a favorable electrode area to solution volume ratio could be obtained. The platinum auxiliary electrode and S.C.E. were separated from the working electrode compartment by a medium size frit.

Spectroelectrochemistry. A gold minigrid optically transparent thin-layer electrode (OTTLE) was used to monitor the spectral changes of mAMSA upon oxidation. Spectropotentiostatic experiments, in which a series of potentials was applied to the cell and a spectrum was recorded after equilibrium had been achieved, were used for determining the formal redox potential ($E^{\circ\prime}$) and number of electrons involved (n) in the redox process. The theory and practice of OTTLE technique have been described in detail [13, 14]. The particular OTTLE used in this study was made of 100 lines/inch gold minigrid, 1 × 2.5 inch quartz slides, and 0.03 inch Teflon spacer. A Hewlett Packard model 8450A UV/VIS spectrometer was used to acquire and record the spectra of mAMSA/mAQDI at the OTTLE upon sequential potential steps. The buffer used was 0.1 M phosphate and 10 mM Tris–HCl, pH 7.5, as a higher ionic concentration was needed to compensate for the cell resistance of OTTLE.

Fluorometric measurements. Fluorescence measurements were performed in a 1-ml, 1-cm quartz cuvette with a Perkin–Elmer model 650–40 fluorescence spectrometer, equipped with a 150 W xenon arc source and a model 3600 data station. The excitation wavelength was set at 400 nm. Uncorrected fluorescence spectra were reported.

Reaction of mAMSA and mAQDI with pDPT275 DNA. The reaction mixtures contained various amounts of mAMSA and Cu(II) in 10 mM Tris–HCl, pH 7.5. They were incubated at room temperature for various times before the addition of 0.74 μg pDPT275 DNA. The mixtures were further incubated for 30 min. After adding 20 μl of a solution containing 50% glycerol (v/v), 40 mM EDTA, and 0.05% bromophenol blue (w/v), the samples were subjected to agarose gel electrophoresis. In some experiments, mAQDI (120 μM) was generated electrochemically in 10 mM Tris–HCl, pH 7.5, with a RVC electrode. The applied potential at the working electrode was set at 0.4 V, about 200 mV more positive than the oxidation peak of mAMSA in this medium. Complete electrolysis was achieved in a time frame (<15 min) in which the irreversible degradation of mAQDI was negligible. Freshly prepared mAQDI was used for the assays of DNA breakage activity.

Agarose gel electrophoresis. Electrophoresis was performed as described by Wong *et al.* [9]. Agarose slab gels (1.1%) were run at 4 V/cm for 14 hr in 40 mM Tris–HCl buffer containing 5 mM sodium acetate and 1 mM EDTA, pH 7.8. After electrophoresis, gels were stained with 1 mg/ml ethidium bromide in the electrophoresis buffer and photographed. The negative films of gels were used for densitometric scannings. The amounts of form II and form III DNA were used to calculate the extents of single-strand and double-strand breaks respectively. The intensities of the form I and form II DNA were appropriately corrected (stainability of form I DNA was 70% of that of form II or form III DNA).

Thin-layer chromatography. Aliquots of 1 ml mAMSA and Cu(II) mixture (100/30 or 30/100 μM/μM) were incubated at room temperature for various times, and 150 μl benzene was then added. The tubes were shaken vigorously for 30 sec and centrifuged; the organic phase was transferred to clean test tubes. A 20-μl aliquot of the benzene extract was spotted on silica gel plates. The plates were developed with 1-butanol plus acetic acid plus water (4:1:1). After chromatography, the separated migration spots were photographed under an ultraviolet illumination (254.6 nm) lamp. The negative films were used in densitometric scanning for quantitation of the migration spots.

Determination of Cu(I) production. The concentrations of Cu(I) produced in the mAMSA–Cu(II) reaction mixtures were determined by titrat-

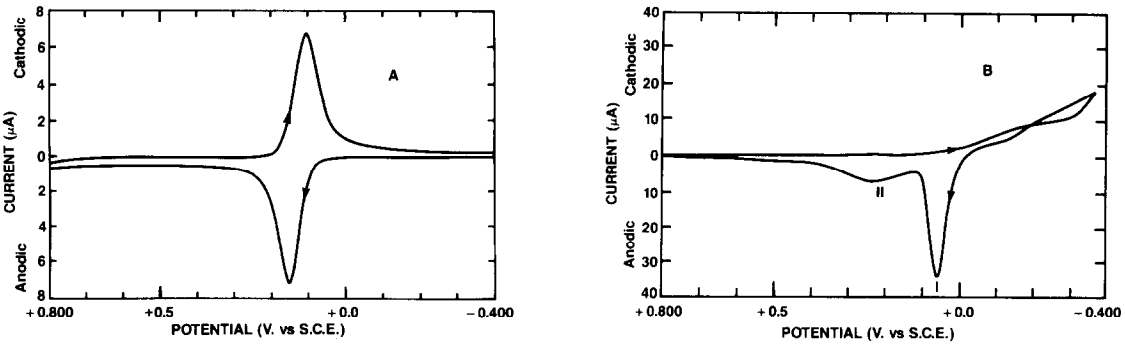

Fig. 1. Cyclic voltammograms of (A) 120 μM mAMSA and (B) 100 mM $CuSO_4 \cdot 5H_2O$ in Tris–HCl buffer, pH 7.5. Peak I probably corresponds to the conversion of the surface bound Cu(O) to Cu(I). Peak II corresponds to the oxidation of a certain Cu(I) species to Cu(II). Conditions are: S.C.E. reference electrode, carbon paste working electrode. scan rate = 100 mV/sec.

ing with bathocuproine as described previously [10]. mAMSA–Cu(II) mixtures (10/30 or 30/10 μM/μM) were incubated at room temperature for various times. Bathocuproine was then added to attain a final concentration of 100 μM. The absorbance at 480 nm was recorded.

RESULTS

Cyclic voltammetric studies of mAMSA and cupric sulfate solutions. A cyclic voltammogram of mAMSA in 10 mM Tris–HCl buffer, pH 7.5, is shown in Fig. 1A. In the potential region between −0.4 and 1.0 V, a well-defined oxidation peak was observed at 0.15 V vs the S.C.E. with the initial scan in the positive direction. Upon scan reversal, a corresponding reduction peak appeared at 0.1 V. The ratio of anodic to cathodic peak current was approximately equal to 1 with no significant change between 5 mV/sec to 500 mV/sec. Figure 1B shows the voltammetric behavior of a $CuSO_4 \cdot 5H_2O$ solution. The ill-defined cathodic response is typical for a bivalent transition metal at the carbon paste electrode in aqueous buffer due to the deposition of reduction product(s) at the electrode surface. Two oxidation peaks can be observed at 0.07 V (peak I) and 0.25 V (peak II) after the initial reduction. Peak I is unusually sharp as compared to Peak II. This suggests that Peak I was a "stripping peak", which probably corresponds to the conversion of the surface bound Cu(0) to Cu(I), whereas Peak II corresponds to the oxidation of a certain Cu(I) species to Cu(II). Since the anodic peak potential of mAMSA falls between the Cu(0)/Cu(I) and Cu(I)/Cu(II) peak, this may suggest that the transfer reaction between mAMSA and Cu(II) to form Cu(I) and mAQDI is probable.

Spectroelectrochemical determination of the formal reduction potential (E°′) and number of electrons transferred (n) of mAMSA. Figure 2 shows a series of absorption spectra of mAMSA observed at a gold minigrid optically transparent thin-layer electrode (OTTLE) at various applied potentials. The four spectra with isosbestic points at 238, 260, 278 and

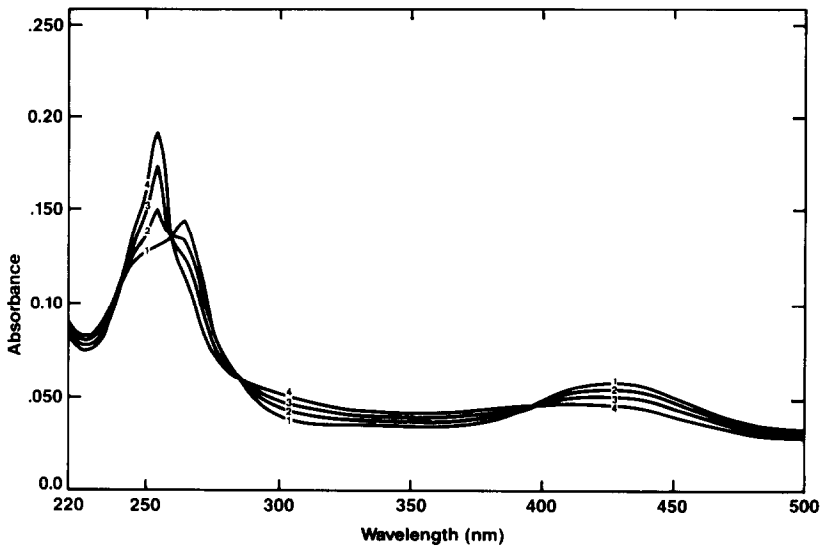

Fig. 2. Spectroelectrochemical response of mAMSA in an OTTLE cell. Curves 1, 2, 3 and 4 represent absorption spectra for mAMSA (120 μM) on an open circuit, 0.14 V, 0.15 V and 0.16 V vs S.C.E. respectively. The solution was 0.1 M phosphate and 10 mM Tris–HCl, pH 7.5.

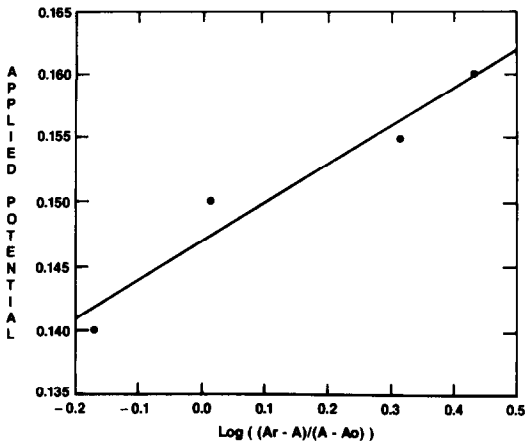

Fig. 3. Nernstian plot based on spectroelectrochemical data. The slope is 0.030 mV and the y-axis intercept is 0.141 V. See text for the designation of A_r, A_o, and A and the significance of the plot.

395 nm represent the transformation of the fully reduced form, mAMSA, to a fully oxidized form via electrooxidation. Since the oxidized mAMSA (spectrum No. 4) has spectral characteristics equivalent to the authentic mAQDI as described previously [10, 15], this confirms that the electrochemical process indeed involves the conversion from mAMSA to mAQDI. The spectra obtained at these potentials were stable for at least 30 min if 5 min elapsed time was allowed for the solution to reach a Nernstian equilibrium. The process was reversible, i.e. mAMSA could be regenerated by re-reduction (data not shown).

Figure 3 shows a Nernstian plot which was constructed based on the spectropotentiostatic data

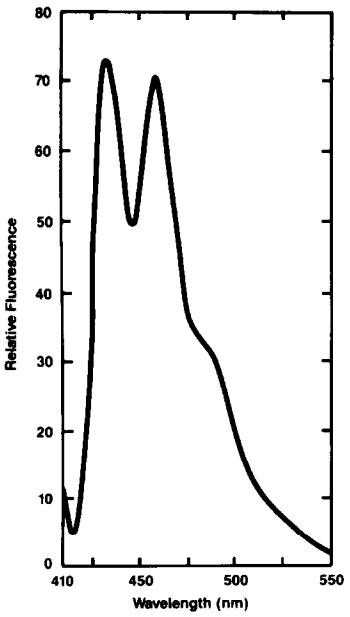

Fig. 4. Fluorescent product produced by aging of mAQDI. Sample contained 120 μM in 1 ml of 10 mM Tris–HCl buffer, pH 7.5. Fluorescence spectrum was recorded after 1 hr of incubation at room temperature.

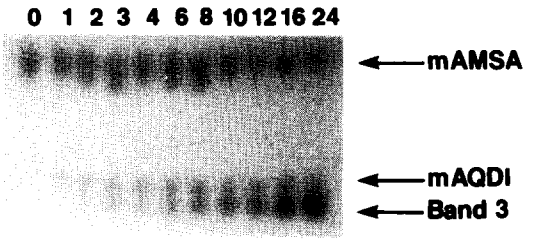

Fig. 5. Thin-layer chromatography of the mAMSA–Cu(II) mixtures. Reaction mixtures contained [mAMSA]/[Cu(II)] = 30 μM/100 μM in 1 ml of 10 mM Tris–HCl buffer. Samples were obtained at different hours of incubation.

obtained from Fig. 2. The Nernst equation states that E_{appl} (applied potential) $= E^{\circ\prime} + 0.059\ V/n \cdot \log (A_r - A)/(A - A_o)$. The applied potential at the OTTLE is plotted against the logarithm of $(A_r - A)/(A - A_o)$ for the mAMSA system. A_r, A_o and A represent the absorbance at 254 nm for the fully reduced form (mAMSA), the fully oxidized form (mAQDI), and the partially oxidized mixture at the designated potential respectively; n designates the number of electrons transferred during the reaction. A slope of 0.030 and a y-axis intercept of 0.141 V were obtained. Therefore, for the redox couple mAMSA/mAQDI, $E^{\circ\prime}$ is 0.141 V and n is 2.

Stability of mAQDI. Cyclic voltammetry and visible absorption spectrometry showed that re-reduction of the mAQDI solution which had been aged for 30 min after electrolysis regenerated about 90% of the initial mAMSA. Increasing time of aging sharply decreased the percentage of mAMSA that could be regenerated. These data suggest that mAQDI may undergo irreversible degradation. Like mAMSA, the freshly prepared mAQDI solution did not exhibit detectable fluorescence. However, aging of mAQDI resulted in the formation of fluorescent product(s) (Fig. 4). The fluorescence intensity increased with the duration of aging. The degradative product displayed the same fluorescence spectrum as the authentic 9-aminoacridine, i.e. a doublet at 430 and 450 nm and a shoulder around 480 nm (excitation at 400 nm). These data, together with thin-layer chromatographic studies (see below), suggest that mAQDI may slowly decompose to form 9-aminoacridine.

Studies on the mAMSA–Cu(II) reaction by thin-layer chromatography. Figure 5 shows that, when an mAMSA–Cu(II) mixture of 30 μM/100 μM was incubated for increasing time, there was a gradual decrease in the amount of mAMSA band (R_f 0.63), which was accompanied by an increase in mAQDI (R_f 0.52) and an additional product designated band 3 (R_f 0.49). All three compounds (mAMSA, mAQDI and band 3) absorbed in the short u.v. region and were nonfluorescent. After prolonged reaction (>40 hr), all the mAMSA in the mixture was degraded and a bright fluorescent band (band 4, R_f 0.63) was observed (data not shown). Band 4 was identified as 9-aminoacridine since it had the same R_f value and fluorescence characteristics as the authentic 9-aminoacridine. Densitometric scanning studies (Fig. 6) show that, in the mAMSA–Cu(II) mixtures of both 30 μM/100 μM and 100 μM/30 μM,

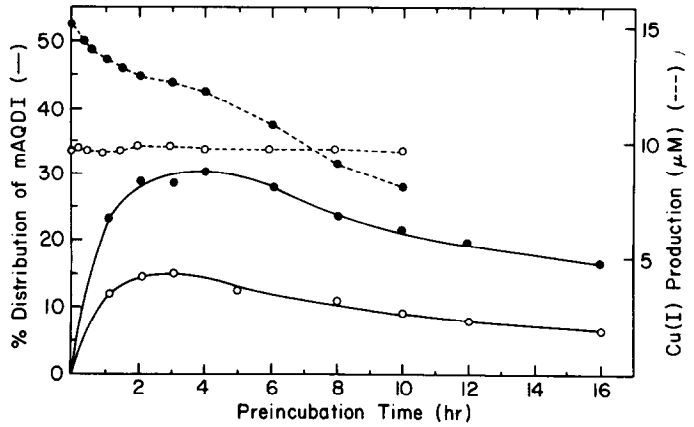

Fig. 6. Kinetic changes of the production of mAQDI and Cu(I). Percent distribution of mAQDI was calculated from densitometric scanning of the TLC patterns obtained from Fig. 5. Cu(I) production was determined by titrating the mAMSA–Cu(II) mixture with bathocuproine. Key: (●) [mAMSA]/[Cu(II)] = 10 μM/30 μM, and (○) 30 μM/10 μM.

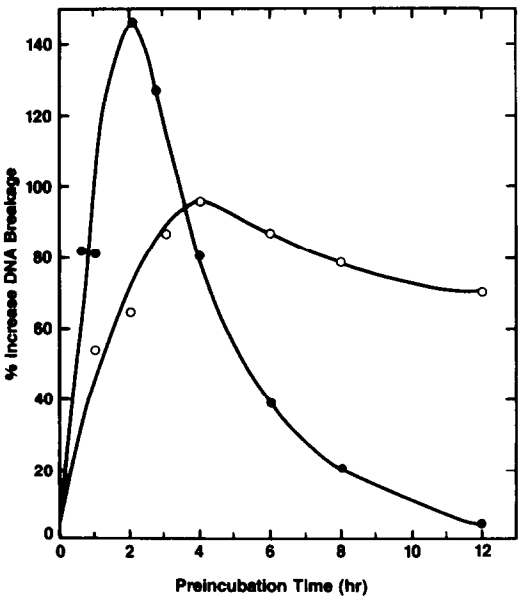

Fig. 7. Kinetic changes of the DNA-breaking activity of the mAMSA–Cu(II) mixture. DNA was added at different times after mixing of mAMSA and Cu(II). Key: (●) [mAMSA]/[Cu(II)] = 10 μM/30 μM, and (○) 30 μM/10 μM.

maximal mAQDI production was obtained after 2 hr of reaction, maintained for up to 4 hr, and then followed by a slight decrease in mAQDI.

In 10 mM Tris–HCl buffer, pH 7.5, mAQDI (obtained from controlled potential electrolysis) was partially (40–50%) converted to band 3 after 2 hr of incubation (data not shown). However, mAQDI was stable in nonaqueous media, such as benzene and ethylacetate, in which hydrolysis could not occur (no degradation of mAQDI could be detected after 12 hr of incubation). This suggests that band 3 may be a hydrolysis product of mAQDI.

Kinetic changes of Cu*(I) production.* Figure 6 shows that, for an mAMSA–Cu(II) mixture of 10 μM/30 μM, Cu(I) production decreased linearly with increasing times of incubation (1–10 hr). However, for a mixture of 30 μM/10 μM, Cu(I) production was maintained constant during the assay period.

Kinetic changes of the DNA breakage activity. When the mAMSA–Cu(II) mixtures were preincubated for various times before assaying for DNA breakage, the breakage activity changed during the time of incubation (Fig. 7). The percent increase in DNA breakage was calculated as $(A - B)/B \times 100$ (A and B are the percentages of form II DNA obtained with or without the preincubation of mAMSA and Cu(II) before assaying for DNA break-

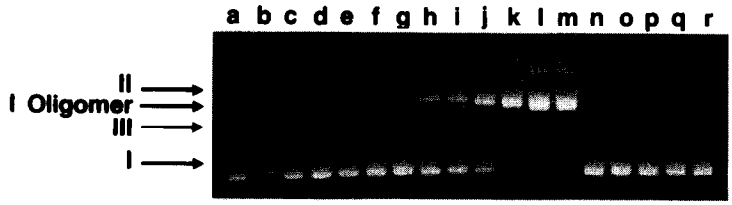

Fig. 8. Agarose gel electrophoretic pattern of ethidium bromide stained pDPT275 DNA after treatment with mAQDI and Cu(I). DNA migrated from top to bottom in the order of decreasing distance of form I, form III, form I oligomer and form II DNA. Lane a: untreated DNA. Lane b: 100 μM mAMSA + 50 μM Cu(II). Lanes c–g: 12.5, 62.5, 125, 187.5 and 250 μM mAQDI. Lane h: 50 μM Cu(I). Lane i–m: 12.5, 62.5, 125, 187.5 and 250 μM mAQDI, in the presence of 50 μM Cu(I). Lanes n–r: 12.5, 62.5, 125, 187.5 and 250 μM mAQDI, in the presence of 50 μM Cu(II). Reaction mixtures were in 10 mM Tris–HCl, pH 7.5, incubated at room temperature for 30 min.

age). For an mAMSA–Cu(II) mixture of 10 μM/30 μM, maximal DNA breakage was obtained at 2 hr, with a subsequent decline at 3–12 hr. For an mAMSA–Cu(II) mixture of 30 μM/10 μM, maximal breakage was achieved at 4 hr and was maintained for 12 hr.

DNA breakage induced by mAQDI in the presence of Cu*(I)*. Figure 8 shows the ethidium bromide stained DNA banding pattern of pDPT275 DNA in an agarose gel. Lane a represents the untreated pDPT275 DNA form I preparation. Lane b shows that treatment of form I DNA with mAMSA (100 μM), in the presence of 50 μM Cu(II), caused a decrease in the banding intensity of form I and a simultaneous increase in that of form II, which indicated single-strand DNA breakage. Treatment with mAQDI at increasing concentrations, alone (12.5 to 250 μM, lanes c–g), or in the presence of 50 μM Cu(II) (lanes n–r), induced no DNA breakage. However, in the presence of 50 μM Cu(I), treatment with mAQDI at increasing concentrations (12.5 to 250 μM, lanes i–m) produced a gradual increase in form II (single-strand breaks) DNA and form III (double-strand breaks) DNA. There was an apparent gradual shift in the production of form III dimer (DNA breakage product obtained from form I dimer) to form III monomer. Cu(I) (50 μM) when used alone (lane h) produced only a small amount of single-strand DNA breakage.

Quantitative analysis by densitometry of the DNA break production was performed. The untreated pDPT275 DNA preparation contained approximately 90–95% form I DNA and 5–10% form II DNA. Form I oligomeric DNA was not considered in the calculation of the percentage DNA distribution. In the presence of 50 μM Cu(II), 100 μM mAMSA produced 42% of form II DNA. This is comparable to the DNA breakage activity reported previously [9]. Figure 9 shows the densitometric scanning results of lanes h–m of Fig. 8. In the presence of 50 μM Cu(I), DNA breakage increased linearly with increasing concentrations of mAQDI (12.5 to 250 μM). A maximum of 66% conversion of form I DNA to form II occurred at 185–250 μM mAQDI. Three to six percent form III DNA was obtained at 125–250 μM mAQDI. When used alone, 50 μM Cu(I) induced 15–18% form II DNA.

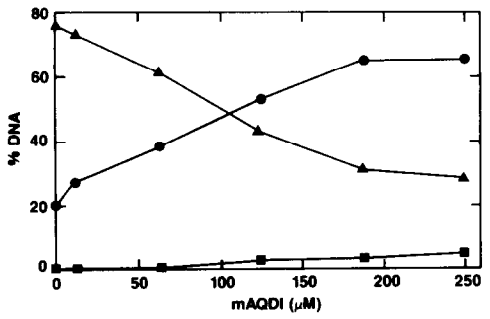

Fig. 9. Percentage distribution of DNA conformational isomers after treatment with mAQDI and Cu(I). Data were obtained from the gel pattern shown in Fig. 8, lanes h–m. DNA was treated with increasing concentrations of mAQDI in the presence of 50 μM Cu(I). Key: (▲) form I DNA; (●) form II DNA; and (■) form III DNA.

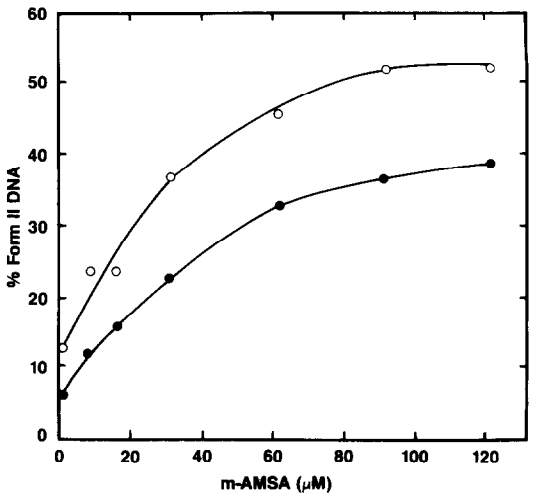

Fig. 10. Synergistic effect of NADPH on DNA breakage. The complete reaction mixture (60 μl) contained 0.74 μg pDPT275 DNA, 60 μM Cu(II) with various concentrations of mAMSA, in the presence (○) or absence (●) of 0.1 mM NADPH; incubation was for 30 min at room temperature.

Degradation of DNA by mAMSA and Cu*(II) in the presence of NADPH*. As shown in Fig. 10, when no mAMSA was present, NADPH (0.1 mM) produced a 5% increase in the Cu(II)-mediated DNA breakage. However, in the presence of increasing concentrations of mAMSA, the effects of NADPH on DNA breakage were enhanced greatly. mAMSA (120 μM), together with Cu(II), induced 35% form II DNA production, whereas with the addition of NADPH, 55% form II DNA was obtained. Hence, addition of NADPH resulted in a 20% increase in the mAMSA–Cu(II)-induced DNA-breakage.

DISCUSSION

By using spectroelectrochemical approaches, we have demonstrated that the redox reaction between mAMSA and mAQDI is a reversible, 2 electron transfer process:

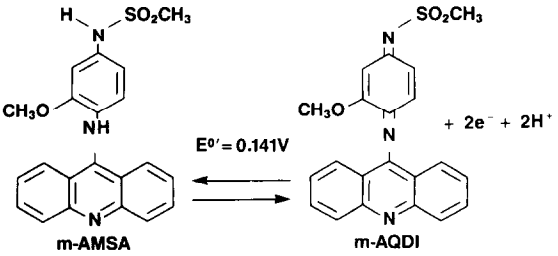

The formal reduction potential of the redox couple mAMSA-mAQDI was 0.141 V. This is sufficient to reduce Cu(II) to Cu(I) (E_p approximately 0.235 V, Fig. 1B, peak II), but not Cu(I) to Cu(O) (E_p approximately 0.065 V, peak I). Hence, the redox reaction between mAMSA and Cu(II) to form mAQDI and Cu(I) was thermodynamically favorable. The presence of isosbestic points (Fig. 2) indi-

cates redox interconversion between two chemical species, mAMSA and mAQDI. No long-lived spectral intermediates were produced during the redox reaction. However, we cannot exclude the possibility that some short-lived intermediates (such as the one electron-transfer radical of mAMSA) which may have formed, but did not accumulate significantly, may have escaped detection.

Three sequential events in the mAMSA–Cu(II) mixture were resolved by thin-layer studies. They are: (1) oxidation of mAMSA by Cu(II) to mAQDI; (2) hydrolysis of mAQDI to band 3; and (3) further decomposition of band 3 to 9-aminoacridine. This reaction sequence is very similar to the *in vivo* metabolism of mAMSA:

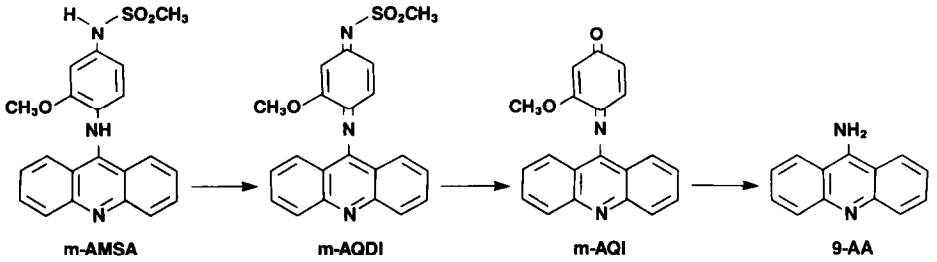

mAMSA is metabolized by the liver microsomal oxygenase system to mAQDI [16–18]. In aqueous solution, mAQDI is hydrolyzed to a quinone imine, 3′ - methoxy - 4′ - (9 - acridinylamino) - 2′, 5 - cyclohexadiene-1′-one (mAQI) which, in turn, is hydrolyzed to yield 9-aminoacridine [19]. At present, no structural studies have been performed to show the chemical nature of band 3. However, like mAQI, band 3 is a hydrolysis product of mAQDI.

Two lines of evidence suggest that the production of both mAQDI and Cu(I) is prerequisite for inducing DNA breakage. First, Cu(I) induced extensive breakage of the pDPT275 DNA, but only in the presence of mAQDI. Neither mAQDI (lanes c–g) nor Cu(I) (lane h), when used alone, produced significant DNA breakage (Fig. 8). Second, the DNA-breaking activity (Fig. 7) was kinetically related to the production of mAQDI and Cu(I). Figure 6 shows that, for an mAMSA–Cu(II) mixture of 1:3, maximal mAQDI production was obtained at 2–4 hr, whereas the production of Cu(I) by the mixture decreased gradually during incubation. Based on these observations, the biphasic DNA breakage activity observed at a 1:3 mAMSA–Cu(II) mixture is predicted. DNA breakage increased as more mAQDI was produced; with longer incubation times, the production of Cu(I) fell as the reducing species (mAMSA) was depleted, leading to a subsequent decrease in breakage activities. At an mAMSA–Cu(II) ratio of 3:1, the production of Cu(I) by the mixture was constant; therefore, no decrease in breakage activity was observed at longer incubation times.

NADPH had a synergistic effect on the mAMSA–Cu(II)-induced DNA-breakage. The effect of NADPH on the enhancement of DNA breakage was probably not mediated through a reduction of Cu(II) to Cu(I). In the absence of mAMSA, NADPH together with Cu(II) induced only a small increase (5%) in form II DNA production, whereas at 120 μM, mAMSA, NADPH and Cu(II) induced a 20% increase in DNA breakage. We have demonstrated that NADPH can reduce mAQDI to mAMSA [10]. It is possible that, with the addition of NADPH, mAMSA is regenerated and, at the same time, the hydrolysis of mAQDI to band 3 is prevented. Thus, NADPH may act as a redox catalyst that enables the DNA-breakage cycle to proceed, until either the reducing equivalents or the DNA are depleted. We have studied the effects of other reducing agents such as $NaBH_4$ on DNA breakage. The results (data not shown) showed that $NaBH_4$ (1 mM), in the presence of Cu(II), induced extensive DNA breakage. Addition of mAMSA further enhanced breakage. This is because $NaBH_4$ is a much stronger reducing agent than NADPH. It may generate enough Cu(I) to induce DNA breakage without the involvement of mAMSA.

In this report we have shown that the mAMSA–Cu(II) redox reaction provides a plausible mechanism for DNA scission. Two characteristics are necessary for DNA scission of mAMSA: first, the drug must be capable of being biochemically activated to mAQDI. Second, mAQDI must couple with Cu(I). Interestingly, mAQDI was considerably more cytotoxic than mAMSA when tested in L1210 cells [17], suggesting that, in cells, mAMSA is activated to mAQDI to produce its cytotoxic activity. mAQDI, still retaining the acridine ring, may intercalate into DNA, and its quinodal moiety may complex with Cu(I) and generate oxygen free radicals to break DNA.

Recent studies have shown that mammalian DNA topoisomerase II is a possible target for mAMSA [20, 21]. mAMSA stimulates the formation of a topoisomerase II–DNA complex which may lead to DNA breakage [22]. Furthermore, we have demonstrated that mAMSA may interact with membrane sulfhydryl-containing cofactors such as glutathione, cysteine and coenzyme A, resulting in the formation of thiol adducts and that these adducts may also intercalate into DNA [23]. Therefore, mAMSA may interact with DNA through several mechanisms which, in combination, may contribute to the DNA breakage activity of mAMSA.

Acknowledgements—We would like to thank Dr. C. L. King for helpful discussions during the course of this study. We thank Drs. C. H. Huang and J. M. Stadel for suggestions in preparing the manuscript and Ms. S. M. Hwang for preparing the pDPT275 DNA. We also thank Ms.

Judy Seaman and Ms. Belinda Proctor for their excellent secretarial assistance.

REFERENCES

1. B. F. Cain and G. J. Atwell, *Eur. J. Cancer* **10**, 539 (1974).
2. S. Legha, M. Keating, G. Bodey, K. McCredie and E. Freireich, *Proc. Am. Ass. Cancer Res.* **21**, 442 (1980).
3. M. L. Slevin, M. S. Shannon, H. G. Prentice, A. J. Goldman and T. A. Lister, *Cancer Chemother. Pharmac.* **6**, 137 (1981).
4. F. Cabanillas, S. S. Legha, G. P. Bodey and E. Freireich, *Blood* **57**, 614 (1981).
5. S. S. Legha, G. R. Blumenschein, A. V. Buzdar, G. N. Hortobagyi and G. P. Bodey, *Cancer Treat. Rep.* **63**, 1961 (1979).
6. M. J. Waring, *Eur. J. Cancer* **12**, 995 (1976).
7. R. K. Ralph, B. Marshall and S. Darkin, *Trends biochem. Sci.* **8**, 212 (1983).
8. L. A. Zwelling, S. Michaelis, L. C. Erickson, R. S. Ungerleider, M. Nichols and W. K. Kohn, *Biochemistry* **20**, 6553 (1981).
9. A. Wong, C-H. Huang and S. T. Crooke, *Biochemistry* **23**, 2939 (1984).
10. A. Wong, C-H. Huang and S. T. Crooke, *Biochemistry* **23**, 2946 (1984).
11. D. B. Clewell and D. R. Helinski, *Biochemistry* **9**, 4228 (1970).
12. W. R. Wilson, J. L. Giesbrecht, R. P. Hill and G. F. Whitmore, *Cancer Res.* **41**, 2809 (1981).
13. T. P. DeAngelis and W. R. Heineman, *J. chem. Educ.* **53**, 594 (1976).
14. W. R. Heineman, *J. chem. Educ.* **60**, 305 (1983).
15. K. Gaudich and M. Przybylski, *Biomed. Mass Spectrom.* **10**, 292 (1983).
16. D. D. Shoemaker, R. L. Cysyk, S. Padmanabhan, H. B. Bhat and L. Malspeis, *Drug Metab. Dispos.* **10**, 35 (1982).
17. D. D. Shoemaker, P. Gormley and L. Malspeis, *Proc. Am. Ass. Cancer Res.* **21**, 308 (1980).
18. D. D. Shoemaker, P. E. Gormley and R. L. Cysyk, *Drug Metab. Dispos.* **8**, 467 (1980).
19. M. N. Khan, A. H. Soloway, R. L. Cysyk and L. Malspeis, *Proc. Am. Ass. Cancer Res.* **21**, 306 (1980).
20. W. E. Ross and M. O. Bradley, *Biochim. biophys. Acta* **654**, 129 (1981).
21. B. Marshall, R. K. Ralph and R. Hancock, *Nucleic Acids Res.* **11**, 4251 (1983).
22. E. M. Nelson, K. M. Tewey and L. F. Liu, *Proc. natn. Acad. Sci. U.S.A.* **81**, 1361 (1984).
23. A. Wong, C. H. Huang and A. W. Prestayko, *Proc. Am. Ass. Cancer Res.* **23**, 7 (1982).